Astron. Astrophys. 335, 303–308 (1998)

ASTRONOMY
AND
ASTROPHYSICS

Heating and acceleration of minor ions in the solar wind

A. Czechowski[1], R. Ratkiewicz[1], J.F. McKenzie[2], and W.I. Axford[2]

[1] Space Research Centre, Polish Academy of Sciences, Bartycka 18A, PL-00716 Warsaw, Poland
[2] Max-Planck-Institut für Aeronomie, Postfach 20, D-37189 Katlenburg-Lindau, Germany

Received 7 November 1997 / Accepted 23 March 1998

Abstract. We make use of the results of a one-ion model of McKenzie et al. (1997) to obtain the critical solution describing the acceleration of a two-ion solar wind. The model includes preferential heating of the heavy ion species and the temperature anisotropy expected if the heating is predominantly due to ion-cyclotron damping. The relationship of the model to the picture emerging from UVCS/SOHO observations is discussed.

Key words: acceleration of particles – polarization – Sun: corona – solar wind

1. Introduction

Recent UVCS/SOHO data (Kohl et al. 1997, Cranmer et al. 1997) show, for the heavy ions exemplified by O^{5+}, very high temperatures reaching $\sim 10^8$ K in the inner corona with large temperature anisotropy ($T_\perp \sim 10^2\, T_\|$). This is in general agreement with the picture suggested by McKenzie et al. (1995, 1997) where plasma heating is taken to be due to dissipation of high frequency waves close to the solar surface. The present work embodies ideas stretching back almost three decades. The idea that the corona could be very hot ($\sim 10^7$ K) was first hinted at by Holzer and Axford (1970) in order to account for high solar wind speeds. Ryan and Axford (1975) explored the consequences of minor ions in the solar wind being heated proportional to their mass. Leer and Axford (1972) extended the two fluid (electron-proton) work of Sturrock and Hartle (1966) to allow for different perpendicular and parallel proton temperatures ($T_\perp \neq T_\|$). This body of work taken together with Bame et al. (1975) and the HELIOS (Marsch et al. 1982) and ISEE observations (Schmidt et al., 1980) to the effect that $T_\perp > T_\|$, $T_i \sim AT_p$, $u_i = u_p + v_A$ lends support to the idea that the ion cyclotron resonant processes would be a natural candidate to account for these observed properties (Axford, 1980).

In the present paper we extend the one-ion treatment of McKenzie et al. (1997) by considering two ion components, the minor component being either the α or O^{5+} (in the latter case the main component is taken to be the ($\alpha + p$) mixture). In parallel to the early work (Yeh 1970, Weber 1973) our treatment exploits the critical structure of the phase space of the stationary bi-ion flow equations using the generalized concept of sonic points in a bi-ion flow including differential streaming (McKenzie et al. 1993). In order to avoid solving the coupled energy and momentum equations we use the proton temperature profiles of McKenzie et al. (1997) and assume the minor component is preferentially heated proportional to its mass (with an extra factor of $K \geq 1$). The acceleration due to waves and the Coulomb friction are taken into account. The case with isotropic temperatures and adiabatic evolution of the wave force, based on McKenzie et al. (1995), was considered in Czechowski et al. (1997).

The published work on the multi-ion solar wind acceleration problem, apart from early isothermal models (Yeh 1970, Weber 1973) or the calculations assuming simple temperature profiles (Leer, Holzer & Shoub 1992), include also, starting from Burgi (1992), the more complete calculations in which the energy transport equations are solved simultaneously with the flow equations, with some assumptions made for the source terms. However, none of those cover the case that we consider, namely the anisotropic temperature profiles and a complete expression for the wave force. The extensive study of Hansteen et al. (1997), while encompassing also the chromosphere, is restricted to the case of isotropic temperatures. Isenberg (1984) included both the wave force and anisotropic temperatures as well as a specific model of the resonant interaction, but his calculations were limited to the region outside 10 R_S, beyond the solar wind critical points. We do not intend to review here the whole field of solar wind acceleration theories but we want to draw attention to interesting recent work by Hu et al. (1997) and Tu and Marsch (1997).

2. The model

We consider the flow along a tube of infinitesimal cross section $A(r)$ starting at the base of the corona. The magnetic field $\mathbf{B}$ is parallel to the flow and the flow tube is directed radially outward. By n_j, $p_{j\perp}$, $p_{j\|}$, m_j, Z_j and u_j we denote the number density, partial pressure (perpendicular or parallel to the $\mathbf{B}$ field), particle mass, electric charge number and the flow speed of the j-th ($j = 1, 2$) ion species; the subscript e denotes the electron component. M_S, R_S are the mass and the radius of the Sun. The magnetic flux and the particle flux through the tube are conserved: $BA = \Phi =$

Send offprint requests to: A. Czechowski

$const, n_j u_j A = J_j = const\,(j = 1, 2), n_e u_e A = J_e = const$. For electrons we assume isotropic temperature T_e and take the zero m_e limit in the momentum equation which then determines the electric field E. The momentum equation for the i-th ion component is ($i = 1, 2$):

$$u_i \frac{du_i}{dr} = -\frac{1}{n_i m_i}\frac{d}{dr}p_{i\|} - \frac{1}{n_i m_i}\left(p_{i\|} - p_{i\perp}\right)\frac{1}{A}\frac{dA}{dr} - \frac{GM_S}{r^2} + \frac{Z_i e}{m_i}E + \sum_{k\neq i}\nu_{ik}\left(u_k - u_i\right)\Psi_{ik} + \frac{F_i}{n_i m_i} \tag{1}$$

in which E is given by

$$E = -\frac{1}{en_e}\nabla p_e \tag{2}$$

In addition there are charge neutrality and zero electric current constraints. The system is closed by assuming that the temperature profiles are prescribed as above and the flow tube area factor is given by the magnetic field model of Banaszkiewicz et al. (1997).

In Eq. (1) ν_{ik} denote the characteristic collision frequencies associated with Coulomb friction between the ion components and Ψ_{ik} are the correction factors as given in Leer et al. (1992). The wave force F_i acting on the i-th ion species ($i = 1, 2$) is given by

$$\frac{F_i}{n_i m_i} = \nabla\left(\frac{p_w}{B^2/4\pi}\left(V_{ph}^2 - u_i^2\right)\right) + \frac{Q_i}{n_i m_i}\frac{1}{V_{ph} - u_i} \tag{3}$$

where p_w is the wave pressure. The first term represents the non-resonant interactions (McKenzie). The second (see Isenberg & Hollweg 1982, 1983, Isenberg 1984) is induced by presence of wave dissipation, including the resonant contribution (McKenzie & Marsch, 1982). The source terms Q_i determine heating of the ion components and the wave dissipation. The latter can be expressed as an equation for the decay of the wave action

$$\frac{1}{A}\frac{d}{dr}\left(A\,2p_w\frac{V_{ph}^2}{V_A^2}\left(V_{ph} - u_m\right)\right) = -\sum_i \frac{Q_i}{1 - \frac{u_i}{V_{ph}}} \tag{4}$$

Here $u_m = \sum_i m_i n_i u_i / \sum_i m_i n_i$ and V_{ph} denotes the phase speed of the waves, given by the dispersion formula

$$\sum_i m_i n_i \left(V_{ph} - u_i\right)^2 = \frac{B^2}{4\pi} \tag{5}$$

We take into account only the outward propagating waves. Eq. (5) corresponds to the cold plasma case. In hot anisotropic plasma the terms proportional to $p_{i\perp} - p_{i\|}$ would appear in the dispersion formula. We decided to keep the cold plasma expression for consistency with McKenzie et al. (1997). The induced error should not be large, because the Alfven speed much exceeds the thermal speeds.

The dispersion formula we use is not applicable in the high frequency region, in particular near the ion-cyclotron frequency. This implies an inconsistency in our model, because the main heating process is assumed to be due to ion-cyclotron resonance. However, in distinction to Isenberg (1984) and Isenberg and Hollweg (1983), the main term in the heat source (Eq. (A1)) is in our model concentrated within ~ 0.35 R$_S$ from the solar surface, so that the description of the outside region should be less affected by the approximation. A consistent treatment of the resonant interaction would require not only a kinetic description of ion-cyclotron damping but also the evolution of the wave spectrum, which is beyond the scope of this model.

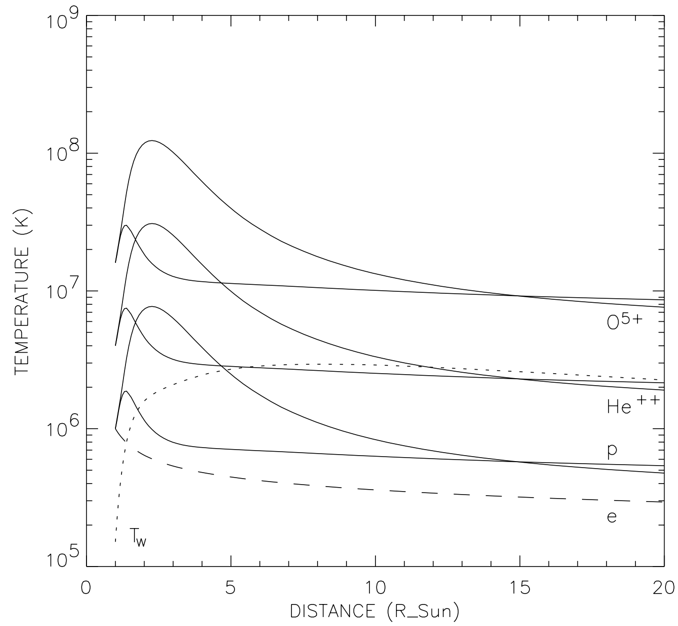

Fig. 1. Temperature profiles $T_p(r), T_\alpha(r), T_{O^{5+}}(r)$ (solid lines), $T_e(r)$ (dashed line) and $T_w(r)$ (dotted line). For the ions both perpendicular (upper lines) and parallel (lower lines) temperatures are shown.

When the evolution of wave action (Eq. (4)) is taken into account, the wave force diverges as $u_m \to V_{ph}$: this is related to the streaming instability. When $Q_i \neq 0$ there is another apparent divergence at $V_{ph} - u_i = 0$. This should not appear in a fully consistent treatment, because the waves which are at rest relative to the i-th component should not contribute to its heating (Q_i should become zero). We simulate this by taking $Q_i = ((V_{ph} - u_i)^2/(V_{ph} - u_m)^2)\tilde{Q}_i(r)$ with $\tilde{Q}_i(r)$ a given function of heliospheric distance. Similar form of Q_i (with power of $V_{ph} - u_i$ dependent on the wave spectrum) was used by Isenberg and Hollweg (1983). The resonant interaction is expected to switch off when relative flow speed $u_2 - u_1$ exceeds a critical value which is lower than the Alfven speed (McKenzie and Marsch, 1982) but we do not include this feature in our approximate expression for the source. However, at the distances where the relative speed becomes comparable with the Alfven speed, the resonant effects are in our model not dominant.

3. Results

The minor (species 2) ions we take to be He^{++} ($J_2/J_1 = 0.05$) or O^{5+} ($J_2/J_1 = 0.5\,10^{-4}$) (in the latter case the major species is the proton-alpha mixture with $u_\alpha = u_p$, $n_\alpha/n_p = 0.05$ and $T_\alpha/T_p = 4$). As explained in Appendix A, the temper-

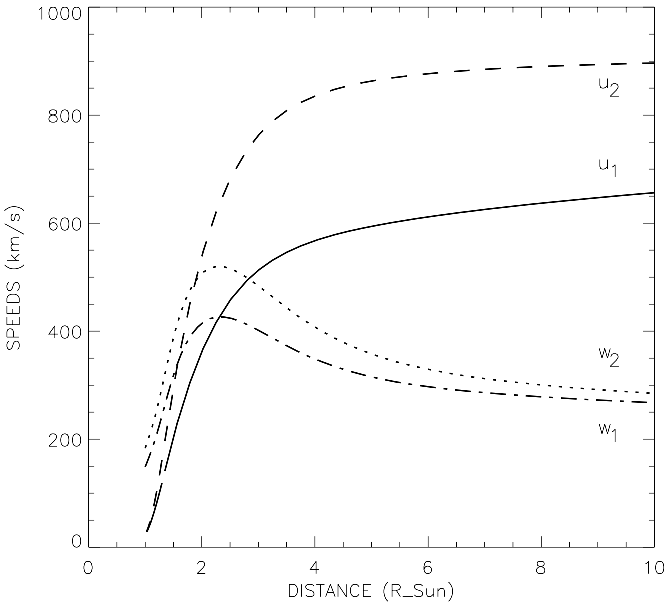

Fig. 2. The flow speeds u_1 (solid line) and u_2 (dashed line) for the $(\mathrm{p}+\alpha, \mathrm{O}^{5+})$ system at $K = 2.0$. Also shown is the combination of the ion thermal (v_{th}) and wave (v_{w}) speeds $w \equiv (v_{\mathrm{th}}^2 + v_{\mathrm{w}}^2)^{1/2}$ for $\mathrm{p}+\alpha$ (dashed-dotted line) and O^{5+} (dotted line).

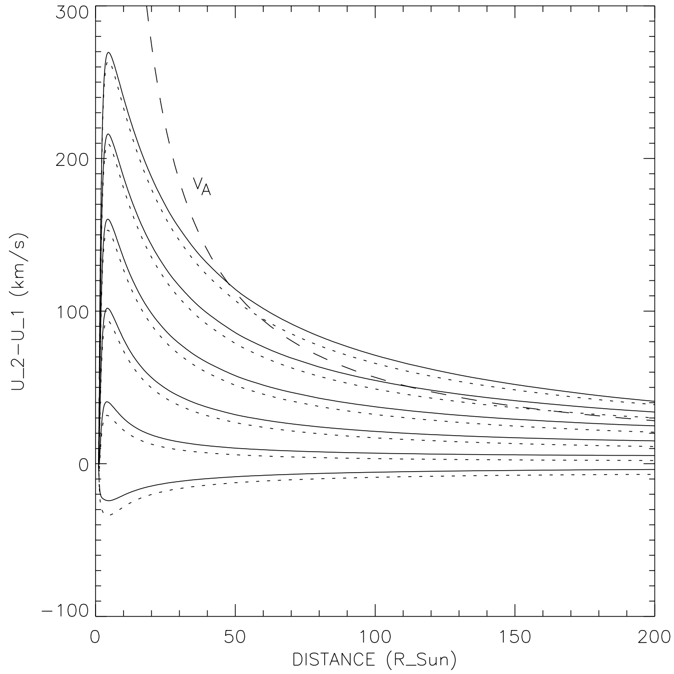

Fig. 3. The relative speed $u_2 - u_1$ for (p, α) (solid line) and $(\mathrm{p}+\alpha, \mathrm{O}^{5+})$ (dotted). The values of the extra heating factor K are (from below) 1.0, 1.2, 1.4, 1.6, 1.8, 2.0. The dashed line is the Alfven speed.

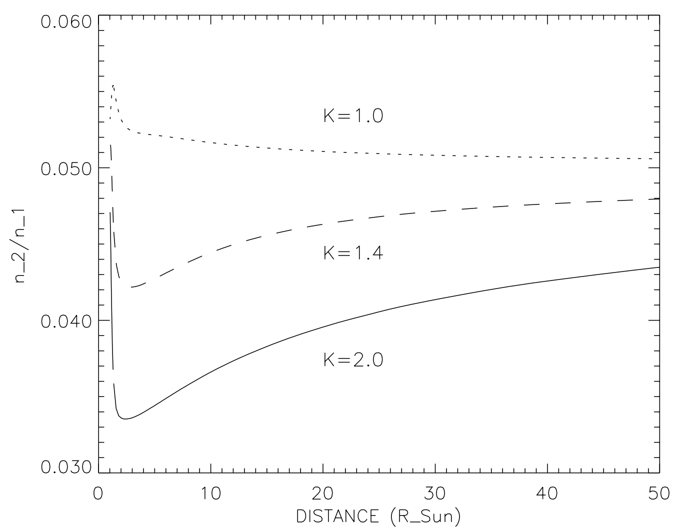

Fig. 4. The density ratio n_α/n_p for $K = 1.0$ (solid line), $K = 1.4$ (dashed line) and $K = 2.0$ (dotted line).

ature profiles are obtained from those derived in the one-ion model of McKenzie et al. (1997) by simple re-scaling. For the ion temperatures this means assuming $T_1(r) = (m_1/m)T(r)$, $T_2(r) = K\,(m_2/m)T(r)$ for both parallel and perpendicular cases ($T(r)$ is the plasma temperature and m the effective ion mass used in the one-ion model). $K \geq 1$ represents additional heating of the heavy ion component; in our calculations we use $K = 1.0, 1.2, 1.4, 1.6, 1.8$ and 2.0. The resulting profiles (with $K = 1.0$ for T_2 curves) are presented in Fig. 1. The limits of the calculation region are 1 $\mathrm{R_S}$ and 1 A.U. The general agreement of the resulting proton flow speed with observations is essentially assured by the input temperature profile for the protons.

Fig. 2 shows the flow speeds corresponding to the critical solution for $(\mathrm{p}+\alpha, \mathrm{O}^{5+})$ case at $K = 1.6$. On the same plot the combinations of the corresponding thermal and wave motion speeds $w_i \equiv (v_{\mathrm{th}i}^2 + v_{\mathrm{w}i}^2)^{1/2}$ responsible for broadening of the spectral lines along the line of sight are shown to compare with the UVCS/SOHO data (Cranmer et al. 1997, Kohl et al. 1997). The observed w_i start to grow from ~ 1.5 $\mathrm{R_S}$ where $w_1 \sim 175$ km/s, $w_2 \sim 75$ km/s and keep increasing up to the outer limit ~ 4 $\mathrm{R_S}$ of the observation region, reaching 250 km/s for hydrogen and 600 km/s for O^{5+}. The O^{5+} flow speed (obtained from Doppler dimming) also starts increasing at ~ 1.5 $\mathrm{R_S}$. The different behaviour of w_i and the flow speeds in our model follows from the assumed form of the heating source (Eq. (A1)), which is concentrated within ~ 0.35 $\mathrm{R_S}$ from the coronal base. Note that the value of T_2/T_1 as inferred from the UVCS/SOHO data can be as high as 90 at ~ 4 $\mathrm{R_S}$.

The relative flow speeds $u_2 - u_1$ are illustrated in Fig. 3. Note that at given K the O^{5+} ions are lagging after the α. This is a consequence of higher value of Z/m of the latter. The Alfven speed is exceeded only for the cases of high excess heating (K=1.8, 2.0) at large distance (50 and 100 $\mathrm{R_S}$, respectively).

The associated changes in density ratios are shown in Fig. 4. Because the heavy ions thermal speeds are high, we cannot expect the mechanism of proton flux regulation (Leer et al., 1992) to apply in this case. Neither is there a significant rise of the alpha density in inner corona (Burgi, 1992).

Fig. 5 illustrates the effects of the wave force and Coulomb friction terms. The wave force contribution to acceleration is

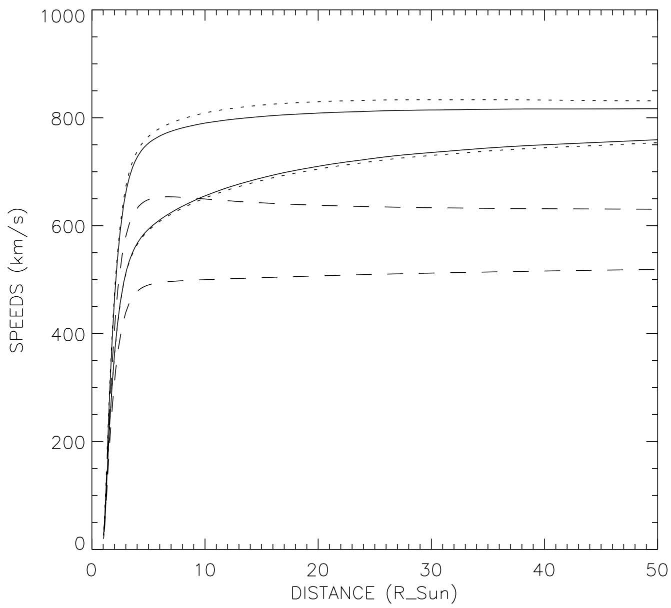

Fig. 5. The proton and alpha (upper line) flow speeds at $K = 1.6$ compared to the cases with no wave force (dashed lines) or no Coulomb friction (dotted lines).

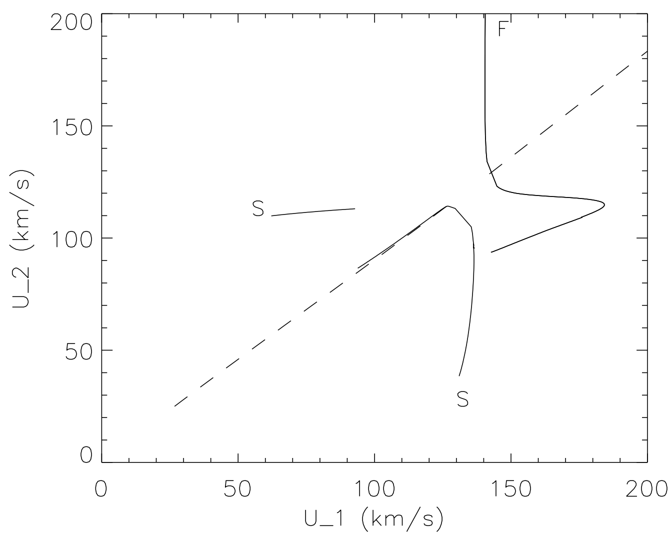

Fig. 6. The (u_1, u_2) plane projection of the critical lines (solid lines) and the critical solution trajectory (dashed line) for the (p, α) system at $K = 1.0$. The solution crosses one of the branches of the slow mode (S) critical line before crossing the critical line (F) corresponding to the fast mode.

seen to be significant. We note that despite the dissipation due to the second term in Q (Eq. (A1)) the relative amplitude of the Alfven waves is above 1 as far as 100 $\mathrm{R_S}$. The maximum value is above 2.0 at 10 $\mathrm{R_S}$.

Figs. 6 and 7 show the (u_1, u_2) plane projection of the critical lines and the critical solution (for clarity only the part $u_1, u_2 \leq 200$ km/s is shown). The slow mode critical curve has two branches, only one of which being crossed by the critical solution. When the minor ion temperature is increased the crossing point moves to another branch. The two critical (crossing) points are close to each other at $\sim 1.35\,\mathrm{R_S}$. See Appendix B for a description of the method of finding the critical solution.

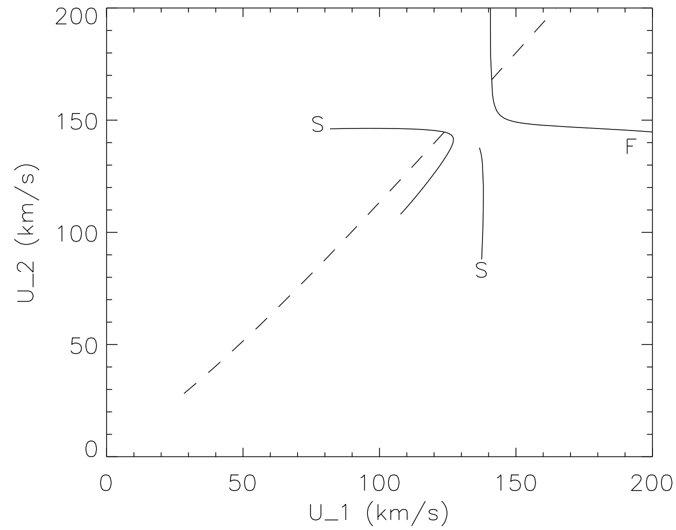

Fig. 7. The (u_1, u_2) plane projection of the critical lines (solid lines) and the critical solution trajectory (dashed line) for the (p, α) system at $K = 1.6$. The solution crossing point on the slow mode critical line moved to another branch.

4. Conclusions

We have presented a model (based on a generalization of McKenzie et al. 1997) which describes the acceleration of α particles and the minor species in high-speed component of the solar wind. The main assumption is that all the heating needed to accelerate the minor species corresponds to the temperature profiles per ion mass equal to those of the protons augmented by an extra factor of $K > 1$. In order to obtain results consistent with observations of helium and minor species in high speed solar wind (differential speed $\sim v_\mathrm{A}$ and high temperatures roughly $\sim$ mass) K must exceed one and perhaps be as large as 2.0. That is, the minor species must be heated more efficiently than the protons. This could be associated with a form of cyclotron resonance with a wave power spectrum which decreases with increasing frequency. As a consequence, the (perpendicular) temperatures of ions in the inner corona ($r \sim 2\,\mathrm{R_S}$) reach 30-50 MK for α particles and 120-200 MK for O^{5+}. Furthermore, if $K > 1.1$ the minor species accelerate faster than the protons and for the preferred value $K = 2.0$ may exceed the proton speed by up to 280 km/s at $r < 20\,\mathrm{R_S}$. The relative flow speed reaches the Alfven speed only at large distance ($r = 50\,\mathrm{R_S}$ for $K = 2$). As a consequence of the specific assumptions of the model, there is no build-up of minor species density in the corona.

Comparing these results with the measurements of UVCS at SOHO (Cranmer et al. 1997, Kohl et al. 1997) we find that, despite some common features (high heavy ion temperatures, flow speeds of ~ 200 km/s reached already at $\sim 2\,\mathrm{R_S}$), there are important differences in detail. The UVCS/SOHO data imply the ratio between O^{5+} and the proton temperatures to be much higher than our upper limit, although the maximum O^{5+} temperature is close to the value used in the model. The shape of the temperature profiles inferred from the observations are quite different from our model. In particular, the rise of temperatures starts apparently not at $1\,\mathrm{R_S}$ but only at $\sim 1.5\,\mathrm{R_S}$ and the peak is not reached within the observation limits (up to $\sim 4\,\mathrm{R_S}$). On the other hand, the preferential heating of the transverse ion motion is confirmed by the analysis of the data (Kohl et al. 1997). It is possible that the ion-cyclotron heating becomes more effective after some minimum distance from the coronal base. It would be worthwhile to explore this possibility in future work so as to obtain a better agreement with the UVCS observations very close to the Sun.

Acknowledgements. Two of us (A.C. and R.R.) acknowledge support of the grant 2 P03C 002 08 from Komitet Badan Naukowych and wish to thank the Max-Planck-Institute fuer Aeronomie in Lindau for hospitality.

Appendix A: the temperature profiles, source terms and area factor

The wave dissipation and plasma heating (perpendicular temperature) are described by the source term (see McKenzie et al. 1997)

$$Q = C_0 \exp -\frac{r-r_0}{H} + C_1 r^{-3+\delta} \tag{A1}$$

with (for the case we use) $r_0 = \mathrm{R_S}$, $H = 0.35\,\mathrm{R_S}$, $\delta = 0.3$ and $C_0 = 0.486\,10^{-6}$, $C_1 = 0.489\,10^{21}$, where the values of C_0 and C_1 are in SI units. The second term in Q represents extended heating. The area factor for the flow tube is based on the magnetic field model of Banaszkiewicz et al. (1997) which consists of a dipole, quadrupole and current sheet, so

$$\frac{1}{A} \sim \frac{2}{r^3} + \frac{3q}{r^5} + \frac{c}{a(a+r)^2} \tag{A2}$$

where $a = 1.5386\,\mathrm{R_S}$ and $q = 1.5$, $c = 1.0$ if r is in units of $\mathrm{R_S}$.

$T_\mathrm{e}(r), T_\mathrm{w}(r), T_\perp(r)$ and $T_\parallel(r)$ denote respectively electron temperature, 'wave temperature' (defined by $p_\mathrm{w} = n\mathrm{k}T_\mathrm{w}$) and the perpendicular and parallel plasma temperatures as obtained from single-ion model. In our calculation $T_\mathrm{e}(r)$, $T_\mathrm{w}(r)$ are unchanged while the ion temperature profiles we assume to be given by

$$T_{1\perp}(r) = \frac{m_1}{m} T_\perp(r) \qquad T_{1\parallel}(r) = \frac{m_1}{m} T_\parallel(r) \tag{A3}$$

$$T_{2\perp}(r) = K\frac{m_2}{m} T_\perp(r) \qquad T_{2\parallel}(r) = K\frac{m_2}{m} T_\parallel(r) \tag{A4}$$

(m is the effective particle mass in the one-ion model, where 5% alpha admixture was assumed). The constant factor $K \geq 1$ allows us to consider the case when T_2/T_1 is larger than the mass ratio m_2/m_1. The resulting temperature profiles are shown in Fig. 1.

To specify the source terms Q_i in the wave force (Eq. (3)) we would need to know the parameters in the energy equations corresponding to the above temperature profiles. Lacking this, we assume that

$$\frac{\tilde{Q}_1}{\rho_1} = \frac{u_1}{u_\mathrm{m}} \frac{Q}{\rho} \qquad \frac{\tilde{Q}_2}{\rho_2} = K\frac{u_2}{u_\mathrm{m}} \frac{Q}{\rho} \tag{A5}$$

where $\rho_i = m_i n_i$, $\rho = \rho_1 + \rho_2$ and Q is given by Eq. (A1). This is approximately consistent with constant $T_{2\perp}(r)/T_{1\perp}(r)$ ratio if the heating equation is of the form

$$\frac{1}{A}\frac{\mathrm{d}(A\mathrm{k}T_{i\perp})}{\mathrm{d}r} = \frac{Q_i}{n_i u_i} + \cdots \tag{A6}$$

Appendix B: the critical solution

After eliminating the electric field from Eq. (1) by using the electron equation the $i = (1,2)$ momentum equations can be written in the form ($i, k = (1,2), i \neq k$)

$$\frac{1}{u_k}\frac{\mathrm{d}u_k}{\mathrm{d}r} = \frac{a_{kk}R_i - a_{ik}R_k}{det(a)} \tag{B1}$$

where

$$a_{kk} = u_k^2 - c_{k\parallel}^2 - \frac{Z_k n_k}{n_\mathrm{e}} c_{ke}^2 - g_{kk} \tag{B2}$$

$$a_{ik} = -\frac{Z_k n_k}{n_\mathrm{e}} c_{ie}^2 - g_{ik} \qquad (i \neq k) \tag{B3}$$

$$R_i = (c_{i\perp}^2 + c_{ie}^2)\frac{1}{A}\frac{\mathrm{d}A}{\mathrm{d}r} - \frac{\mathrm{d}}{\mathrm{d}r}(c_{i\parallel}^2 + c_{ie}^2) - \frac{G\mathrm{M_S}}{r^2} + \nu_{ik}(u_k - u_i)\Psi_{ik} + g_{i0} \tag{B4}$$

We use $c_{i\parallel}^2 = \mathrm{k}T_{i\parallel}/m_i$, $c_{i\perp}^2 = \mathrm{k}T_{i\perp}/m_i$, $c_{ie}^2 = Z_i\mathrm{k}T_\mathrm{e}/m_i$ and write the wave force as

$$\frac{F_i}{n_i m_i} = g_{i0} + g_{i1}\frac{1}{u_1}\frac{\mathrm{d}u_1}{\mathrm{d}r} + g_{i2}\frac{1}{u_2}\frac{\mathrm{d}u_2}{\mathrm{d}r} \tag{B5}$$

The explicit form of the coefficients g_{ik} can be obtained from Eq. (3).

The system Eq. (B1) is singular at $det(a) = 0$ unless the numerators vanish. The singularity appears when the condition for existence of stationary waves is met for one of the compound modes of the system (McKenzie et al. 1993). For the stationary flow equations under consideration this singularity (and the critical point structure) depends on the formulation: the manifold $det(a) = 0$ would be different if, instead of temperature, we would specify the entropy profiles because the expressions for the sound speeds would be modified.

In the (u_1, u_2, r) space the $det(a) = 0$ surface consists of two parts corresponding to the two eigenvalues (slow and fast modes) of the matrix a. Acceleration from subsonic to supersonic speeds requires the solution to cross through each. This is possible provided that the numerators on the right hand side of the Eq. (B1) vanish which defines the critical curves on the respective $det(a) = 0$ surface sheets. In our approach the critical solution is constructed by first finding (numerically) the two critical lines and then searching for the pair of points on them that can be linked by a solution trajectory. We use the dummy time variable τ such that $\mathrm{d}r/\mathrm{d}\tau = det(a)$ to re-formulate the problem as the 3-dimensional autonomous system with the critical line singularities becoming the lines of fixed points. The relevant segments of the critical lines consist of the saddle point type critical points and the solution crosses them along the separatrix directions, so that integration away from the critical lines is stable.

References

Axford W.I., 1980, Very Hot Plasmas in the Solar System, in: Highlights of Astronomy, ed. P.A. Wayman, Vol.5, 351-359

Bame S.J., Asbridge J.R., Feldman W.C., Gary S.P., Montgomery M.D., 1975, Geophys. Res. Lett. 2, 373-375

Banaszkiewicz M., Axford W.I., McKenzie J.F., 1997, An Analytic Solar Magnetic Field model, Astron.& Astrophys. (submitted)

Burgi A., 1992, Journ. Geophys. Res. 97, 3137-3150

Cranmer, S.R., Field, G.B. and Kohl, J.L., 1997, The Impact of UVCS/SOHO Observations on Models of Ion-Cyclotron Resonance Heating of the Solar Corona, presented at 10th Cambridge Cool Stars Meeting, July 1997

Czechowski, A., Ratkiewicz, R., McKenzie, J.F., Axford, W.I., 1997, Adv. Space Res. 20, 43-46

Hansteen, V.H., Leer E., Holzer T.H., 1997, Ap.J. 482, 498-509

Holzer T.E., Axford W.I., 1970, Ann. Rev. Astron. Astrophys. 8, 31-60

Hu Y.Q., Esser R., Habbal S.R., 1997, Journ. Geophys. Res. 102, 14661-14676

Isenberg P.A., 1984, Journ. Geophys. Res. 89, 6613-6622

Isenberg P.A., Hollweg J.V., 1982, Journ. Geophys. Res. 87, 5023-5029

Isenberg P.A., Hollweg J.V., 1983, Journ. Geophys. Res. 88, 3923-3935

Kohl J.L. et al., 1997, UVCS/SOHO empirical determinations of anisotropic velocity distributions in the solar corona, Ap.J. Letters (submitted)

Leer E., Axford W.I., 1972, Solar Physics 23, 238-250

Leer E., Holzer T.E., Shoub E.C., 1992, Journ. Geophys. Res. 97, A6, 8183-8201

Marsch E., Muhlhauser K.-H., Schwenn R., Rosenbauer H., Pilipp W., Neubauer F.M., 1982, Journ. Geophys. Res. 87, 52-72

McKenzie J.F., Marsch E., 1982, Astr. Space Sci. 81, 295-314

McKenzie J.F., Marsch E., Baumgartel K., Sauer K., 1993, Ann. Geophys. 11, 341-353

McKenzie J.F., 1994, Journ. Geophys. Res. 99, A2, 2585-2586

McKenzie J.F., Banaszkiewicz M., Axford W.I., 1995, Astron.& Astrophys., L45-L48

McKenzie J.F., Banaszkiewicz M., Axford W.I., 1997, Geophys. Res. Lett. 24, 2877-2880

Ryan, J.M. and Axford, W.I., 1975, J. Geophys. 41, 221-232

Schmidt W.K.H., Rosenbauer H., Shelly E.G., Geiss J., 1980, Geophys. Res. Lett. 7, 697-700

Sturrock P.A., Hartle R.E., 1966, Phys. Rev. Lett. 16, 628-631

Tu C.-Y., Marsch E., 1997, Solar Physics 171, 363-391

Weber E.J., 1973, Astr. Space Sci. 20, 391-400, 401-415

Yeh T., 1970, Planet. Space Sci. 18, 199-215